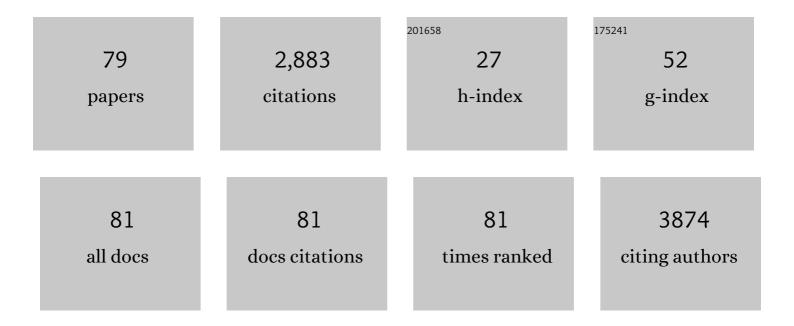
## Ki Chul Kim

List of Publications by Year in descending order

Source: https://exaly.com/author-pdf/6874001/publications.pdf Version: 2024-02-01



КІ С НІЛІ КІХ

#	Article	IF	CITATIONS
1	Dopant-dependent thermoelectric performance of indoloindole-selenophene based conjugated polymer. Chemical Engineering Journal, 2022, 431, 133779.	12.7	13
2	Strategic Design for Sumaneneâ€Derived Organic Cathodes with Tailored Redox Activity. Advanced Theory and Simulations, 2022, 5, .	2.8	1
3	Highly CO-Selective Mixed-Matrix membranes incorporated with Ag Nanoparticle-Impregnated MIL-101 Metal–Organic frameworks. Chemical Engineering Journal, 2022, 435, 134803.	12.7	8
4	Development of computational design for reliable prediction of dielectric strengths of perfluorocarbon compounds. Scientific Reports, 2022, 12, 7027.	3.3	3
5	Modulation of Backbone Architecture to Design Structurally Durable Tetracyanoquinodimethane Derivatives with High Redox Activity. ACS Applied Energy Materials, 2022, 5, 7791-7801.	5.1	0
6	Mechanistic Mapping of Ozone-Dosed Al <sub>2</sub> O <sub>3</sub> Atomic Layer Deposition Half-Cycles. Industrial & Engineering Chemistry Research, 2022, 61, 9695-9702.	3.7	1
7	Effective Nitrogen Incorporation for Highâ€Potential Anthracene Cathodes with Conjugated Frameworks. Advanced Theory and Simulations, 2022, 5, .	2.8	2
8	Toward coupling of electrochemical redox properties with electrostatic potential surfaces tailored by dopant architectures for pyrenetetrone. Energy Storage Materials, 2021, 35, 610-619.	18.0	15
9	Solid-state facilitated transport membrane for CO/N2 separation based on PHMEP-co-PAA comb-like copolymer: Experimental and molecular simulation study. Journal of Membrane Science, 2021, 620, 118939.	8.2	9
10	Tailoring Impact of Carbonyl Functionalities on Electrochemical Redox Properties of Anthraquinone. Journal of Physical Chemistry C, 2021, 125, 8208-8215.	3.1	3
11	Unexpected Electrochemical Behavior of Crown-Based Organic Compounds for Lithium-Ion Battery Cathodes. Industrial & Engineering Chemistry Research, 2021, 60, 7764-7774.	3.7	0
12	Tailored Design of Electrochemically Degradable Anthraquinone Functionality toward Organic Cathodes. ACS Applied Materials & Interfaces, 2021, 13, 35729-35738.	8.0	7
13	Synergistic passivation of MAPbI3 perovskite solar cells by compositional engineering using acetamidinium bromide additives. Journal of Energy Chemistry, 2021, 59, 755-762.	12.9	21
14	Unraveling Threeâ€Stage Discharging Behaviors of Bioâ€Inspired Organic Cathode Materials. Advanced Functional Materials, 2021, 31, 2105285.	14.9	10
15	Ambient-air fabrication of stable mixed cation perovskite planar solar cells with efficiencies exceeding 22% using a synergistic mixed antisolvent with complementary properties. Nano Energy, 2021, 89, 106387.	16.0	14
16	Cu(I)-incorporation strategy for developing styrene selective adsorbents. Chemical Engineering Journal, 2021, 425, 130601.	12.7	8
17	Unraveling Threeâ€Stage Discharging Behaviors of Bioâ€Inspired Organic Cathode Materials (Adv. Funct.) Tj Eī	<sup>-</sup> Qq110.78	34314 rgBT
18	Conjugacy of organic cathode materials for high-potential lithium-ion batteries: Carbonitriles versus	18.0	33

quinones. Energy Storage Materials, 2020, 24, 237-246.

18.0 33

#	Article	IF	CITATIONS
19	Improvement of Electrical Conductivity in Conjugated Polymers through Cascade Doping with Smallâ€Molecular Dopants. Advanced Materials, 2020, 32, e2005129.	21.0	26
20	Molecular Simulation Study on Factors Affecting Carbon Dioxide Adsorption on Amorphous Silica Surfaces. Journal of Physical Chemistry C, 2020, 124, 12580-12588.	3.1	9
21	Influence of a UV-ozone treatment on amorphous SnO2 electron selective layers for highly efficient planar MAPbI3 perovskite solar cells. Journal of Materials Science and Technology, 2020, 59, 195-202.	10.7	28
22	Physisorption and Chemisorption of SF6 by Transition Metal-Porphyrin Structure Embedded on Graphene Surface with Different Hapticities. Journal of the Korean Physical Society, 2020, 76, 1001-1004.	0.7	1
23	Unveiled Understanding on Thermodynamic Mechanisms of Atomic Layer Deposition Based on Trimethylaluminum and Water Precursors. Industrial & Engineering Chemistry Research, 2020, 59, 13325-13332.	3.7	6
24	Electrochemical Characteristics of Cyanoquinones as Organic Cathodes for High-Potential Sodium-Ion Batteries. ACS Sustainable Chemistry and Engineering, 2020, 8, 11328-11336.	6.7	15
25	Insights on Redox Properties of Sumanene Derivatives for High-Performance Organic Cathodes. ACS Applied Materials & Interfaces, 2020, 12, 8333-8341.	8.0	10
26	Enhanced Lithium Storage of an Organic Cathode via the Bipolar Mechanism. ACS Applied Energy Materials, 2020, 3, 3728-3735.	5.1	18
27	Crucial role of cyanides for high-potential electrochemical reduction reaction. Energy Storage Materials, 2020, 29, 140-148.	18.0	14
28	Electrochemical Energy Storage Capability of Pyrenetetrone Derivatives Tailored by Nitrogen Dopants. Journal of Physical Chemistry C, 2020, 124, 10815-10822.	3.1	5
29	Li-Binding Thermodynamics and Redox Properties of BNOPS-Based Organic Compounds for Cathodes in Lithium-Ion Batteries. ACS Applied Materials & Interfaces, 2019, 11, 31972-31979.	8.0	11
30	Well-dispersed carbon nanotube/polymer composite films and application to electromagnetic interference shielding. Journal of Industrial and Engineering Chemistry, 2019, 80, 190-196.	5.8	21
31	Pyrenetetrone Derivatives Tailored by Nitrogen Dopants for High-Potential Cathodes in Lithium-Ion Batteries. IScience, 2019, 21, 206-216.	4.1	14
32	Improving the Understanding of the Redox Properties of Fluoranil Derivatives for Cathodes in Sodiumâ€ion Batteries. ChemSusChem, 2019, 12, 4968-4975.	6.8	15
33	Synthesis, structure and gas separation properties of ethanol-soluble, amphiphilic POM-PBHP comb copolymers. Polymer, 2019, 180, 121700.	3.8	5
34	Unveiled correlations between electron affinity and solvation in redox potential of quinone-based sodium-ion batteries. Energy Storage Materials, 2019, 19, 242-250.	18.0	32
35	Effects of thermal shrinkage temperatures and comonomers on thermal shrinkage of uniaxially-stretched PET copolymer films: a molecular dynamics simulation approach. New Journal of Chemistry, 2018, 42, 4991-4997.	2.8	2
36	Fe–Porphyrin-like Nanostructures for Selective Ammonia Capture under Humid Conditions. Journal of Physical Chemistry C, 2018, 122, 2046-2052.	3.1	7

#	Article	IF	CITATIONS
37	Density Functional Theory Modeling-Assisted Investigation of Thermodynamics and Redox Properties of Boron-Doped Corannulenes for Cathodes in Lithium-Ion Batteries. Journal of Physical Chemistry C, 2018, 122, 10675-10681.	3.1	20
38	Boron-doped coronenes with high redox potential for organic positive electrodes in lithium-ion batteries: a first-principles density functional theory modeling study. Journal of Materials Chemistry A, 2018, 6, 10111-10120.	10.3	22
39	Molecular dynamics simulation study on the structural properties of poly (ethylene terephthalate) under uniaxial extension and thermal shrinkage processes. Current Applied Physics, 2018, 18, 19-26.	2.4	4
40	A review on design strategies for metal hydrides with enhanced reaction thermodynamics for hydrogen storage applications. International Journal of Energy Research, 2018, 42, 1455-1468.	4.5	56
41	Electrochemical and electronic properties of nitrogen doped fullerene and its derivatives for lithium-ion battery applications. Journal of Energy Chemistry, 2018, 27, 528-534.	12.9	36
42	Design strategies for metal-organic frameworks selectively capturing harmful gases. Journal of Organometallic Chemistry, 2018, 854, 94-105.	1.8	34
43	Electrochemical Properties of Boronâ€Doped Fullerene Derivatives for Lithiumâ€Ion Battery Applications. ChemPhysChem, 2018, 19, 753-758.	2.1	37
44	Application of DFT-based machine learning for developing molecular electrode materials in Li-ion batteries. RSC Advances, 2018, 8, 39414-39420.	3.6	96
45	Observation of Olefin/Paraffin Selectivity in Azo Compound and Its Application into a Metal–Organic Framework. ACS Applied Materials & Interfaces, 2018, 10, 27521-27530.	8.0	26
46	Instantaneous Detection of Trichlorinated Carbon via Photo-Induced Electron Transfer toward Chemosensor for Toxic Organochlorides. ACS Sensors, 2018, 3, 1831-1837.	7.8	8
47	Density Functional Theory – Machine Learning Approach to Analyze the Bandgap of Elemental Halide Perovskites and Ruddlesdenâ€Popper Phases. ChemPhysChem, 2018, 19, 2559-2565.	2.1	27
48	Systematic Molecular Design of Ketone Derivatives of Aromatic Molecules for Lithiumâ€lon Batteries: Firstâ€Principles DFT Modeling. ChemSusChem, 2017, 10, 1584-1591.	6.8	44
49	Design Strategies for Promising Organic Positive Electrodes in Lithium-Ion Batteries: Quinones and Carbon Materials. Industrial & Engineering Chemistry Research, 2017, 56, 12009-12023.	3.7	49
50	Enhanced Selectivity for CO <sub>2</sub> Adsorption on Mesoporous Silica with Alkali Metal Halide Due to Electrostatic Field: A Molecular Simulation Approach. ACS Applied Materials & Interfaces, 2017, 9, 31683-31690.	8.0	14
51	Computational screening of functional groups for capture of toxic industrial chemicals in porous materials. Physical Chemistry Chemical Physics, 2017, 19, 31766-31772.	2.8	1
52	Self-polymerized dopamine as an organic cathode for Li- and Na-ion batteries. Energy and Environmental Science, 2017, 10, 205-215.	30.8	253
53	Blends of poly(3-alkylthiophene) and [6,6]-phenyl-C61-butyric acid methyl ester for organic photovoltaic cell applications: Multi-scale modeling approach. Computational Materials Science, 2017, 126, 299-307.	3.0	2
54	Thermodynamic and redox properties of graphene oxides for lithium-ion battery applications: a first principles density functional theory modeling approach. Physical Chemistry Chemical Physics, 2016, 18, 20600-20606.	2.8	39

#	Article	IF	CITATIONS
55	Molecular Dynamics Simulations of Aldol Condensation Catalyzed by Alkylamine-Functionalized Crystalline Silica Surfaces. Journal of the American Chemical Society, 2016, 138, 7664-7672.	13.7	44
56	Selective dynamic separation of Xe and Kr in Co-MOF-74 through strong binding strength between Xe atom and unsaturated Co2+ site. Microporous and Mesoporous Materials, 2016, 236, 284-291.	4.4	52
57	Isomorphous Substitution of Copper in Nickel Phosphate and Their Separation of Propylene Over Propane. Journal of Nanoscience and Nanotechnology, 2016, 16, 9141-9148.	0.9	3
58	Applicability of using CO2 adsorption isotherms to determine BET surface areas of microporous materials. Microporous and Mesoporous Materials, 2016, 224, 294-301.	4.4	112
59	First-Principles Density Functional Theory Modeling of Li Binding: Thermodynamics and Redox Properties of Quinone Derivatives for Lithium-Ion Batteries. Journal of the American Chemical Society, 2016, 138, 2374-2382.	13.7	194
60	Functionalized Fullerenes in Water: A Closer Look. Environmental Science & Technology, 2015, 49, 2147-2155.	10.0	15
61	High-Density Lithium-Ion Energy Storage Utilizing the Surface Redox Reactions in Folded Graphene Films. Chemistry of Materials, 2015, 27, 3291-3298.	6.7	78
62	Computational Screening of Metal Catecholates for Ammonia Capture in Metal–Organic Frameworks. Industrial & Engineering Chemistry Research, 2015, 54, 3257-3267.	3.7	27
63	Modeling Water and Ammonia Adsorption in Hydrophobic Metal–Organic Frameworks: Single Components and Mixtures. Journal of Physical Chemistry C, 2014, 118, 1102-1110.	3.1	57
64	Computational Study of Propylene and Propane Binding in Metal–Organic Frameworks Containing Highly Exposed Cu <sup>+</sup> or Ag <sup>+</sup> Cations. Journal of Physical Chemistry C, 2014, 118, 9086-9092.	3.1	21
65	Crystal structures and thermodynamic investigations of NaSc(BH <sub>4</sub> ) <sub>4</sub> from firstâ€principles calculations. International Journal of Quantum Chemistry, 2013, 113, 119-124.	2.0	6
66	Computational Screening of Functional Groups for Ammonia Capture in Metal–Organic Frameworks. Langmuir, 2013, 29, 1446-1456.	3.5	49
67	Validation of the reaction thermodynamics associated with NaSc(BH4)4 from first-principles calculations: Detecting metastable paths and identifying the minimum free energy path. Journal of Chemical Physics, 2012, 137, 084111.	3.0	4
68	Predictions of Sulfur Resistance in Metal Membranes for H2 Purification Using First-Principles Calculations. Industrial & Engineering Chemistry Research, 2012, 51, 301-309.	3.7	6
69	An Extended Charge Equilibration Method. Journal of Physical Chemistry Letters, 2012, 3, 2506-2511.	4.6	253
70	High Propene/Propane Selectivity in Isostructural Metal–Organic Frameworks with High Densities of Open Metal Sites. Angewandte Chemie - International Edition, 2012, 51, 1857-1860.	13.8	392
71	Examining the robustness of first-principles calculations for metal hydride reaction thermodynamics by detection of metastable reaction pathways. Physical Chemistry Chemical Physics, 2011, 13, 21520.	2.8	14
72	Large-scale screening of metal hydrides for hydrogen storage from first-principles calculations based on equilibrium reaction thermodynamics. Physical Chemistry Chemical Physics, 2011, 13, 7218.	2.8	30

#	Article	lF	CITATIONS
73	New fundamental experimental studies on α-Mg(BH4)2 and other borohydrides. Journal of Alloys and Compounds, 2011, 509, S688-S690.	5.5	29
74	Crystal Structures and Thermodynamic Investigations of LiK(BH <sub>4</sub> ) <sub>2</sub> , KBH <sub>4</sub> , and NaBH <sub>4</sub> from First-Principles Calculations. Journal of Physical Chemistry C, 2010, 114, 678-686.	3.1	56
75	Predicting impurity gases and phases during hydrogen evolution from complex metal hydrides using free energy minimization enabled by first-principles calculations. Physical Chemistry Chemical Physics, 2010, 12, 9918.	2.8	20
76	AZn2(BH4)5(A = Li, Na) and NaZn(BH4)3: Structural Studies. Journal of Physical Chemistry C, 2010, 114, 19127-19133.	3.1	53
77	Assessing nanoparticle size effects on metal hydride thermodynamics using the Wulff construction. Nanotechnology, 2009, 20, 204001.	2.6	127
78	New approach for nanoscale morphology of polymer solar cells. Solar Energy Materials and Solar Cells, 2008, 92, 1188-1191.	6.2	14
79	Unveiled Correlations between Electron Affinity and Solvation in Redox Potential of Quinone-Based Sodium-Ion Batteries. SSRN Electronic Journal, 0, , .	0.4	1